Proceedings of the 28th IEEE
EMBS Annual International Conference
New York City, USA, Aug 30-Sept 3, 2006

Non-Invasive Respiration Rate Estimation Using Ultra-Wideband Distributed Cognitive Radar System

Yifan Chen[1], Erry Gunawan[1], Kay Soon Low[1], Yongmin Kim[2], Cheong Boon Soh[1], A. Rahim Leyman[3], and Lin Lin Thi[1]

[1]Biomedical Engineering Research Centre, Nanyang Technological University, Singapore, 637553

[2]Department of Bioengineering, University of Washington, Seattle, WA 98195, USA

[3]Institute for Inforcomm Research, A*STAR, Singapore, 119613

Abstract – **It has been shown that remote monitoring of pulmonary activity can be achieved using ultra-wideband (UWB) systems, which shows promise in home healthcare, rescue, and security applications. In this paper, a geometry-based statistical channel model is developed for simulating the reception of UWB signals in the indoor propagation environment. This model enables replication of time-varying multipath profiles due to the displacement of a human chest. Subsequently, a UWB distributed cognitive radar system (UWB-DCRS) is developed for the robust detection of chest cavity motion and the accurate estimation of respiration rate. The analytical framework can serve as a basis in the planning and evaluation of future measurement programs.**

I. Introduction

Vital-sign monitoring is a very important application due to a variety of reasons. Firstly, the rapid aging of our society creates new demands of providing adequate and effective healthcare. Secondly, vital sensing could be used in home monitoring for sleep apnea in both infants and adults [1]. Thirdly, more people suffer from chronic health conditions including heart disease, lung disorders, and diabetes. Consequently, there is a growing demand for devices that allow out-of-hospital monitoring of health parameters. The commercial products that exist in the market have a common drawback: a sensor has to be tightly fixed on the user's body. An ideal solution is thus to implement a non-invasive sensing system that does not require any contact to the user. In previous works, the use of ultra-wideband (UWB) radar has been suggested for unobtrusive monitoring of patient's vital signs [2], [3]. UWB radar transmits short impulses with pulse duration ranging from sub-nanoseconds to a few nanoseconds. Due to the high resolution of UWB signals, the expansion of the chest cavity and the heart beat will cause noticeable variations to the channel multipath profile, which can be exploited to estimate the respiration and heart rates. The main advantages of UWB radar for real-life implementation of home healthcare application include [2], [3]: (1) high material-penetration capability; (2) low electromagnetic interference as well as lower specific absorption rates; (3) good immunity against multipath interference, thereby enhancing measurement reliability; and (4) low energy consumption and diminished sizes of device.

In [2] and [3], no detailed analysis was given regarding the propagation channel models, elaborate system architectures, and signal processing algorithms. In this paper, a generic framework is presented for the development of UWB systems for remote vital sensing. In the initial stage, we will only focus on the detection and estimation of respiration rates under the scenarios where human movements are not an issue, e.g., monitoring elderly or infant overnight, home healthcare of immobile patients. We first propose a geometry-based statistical model for simulating the non-stationary propagation channel due to the presence of human object. The model is derived in terms of several key parameters of the site-specific features of indoor environment. Next, a UWB distributed cognitive radar system (UWB-DCRS) is developed to enhance the measurement reliability. Different modules of the system architecture are described in detail and a set of important parameters are recognized through the analysis, which are useful for the planning of future measurements.

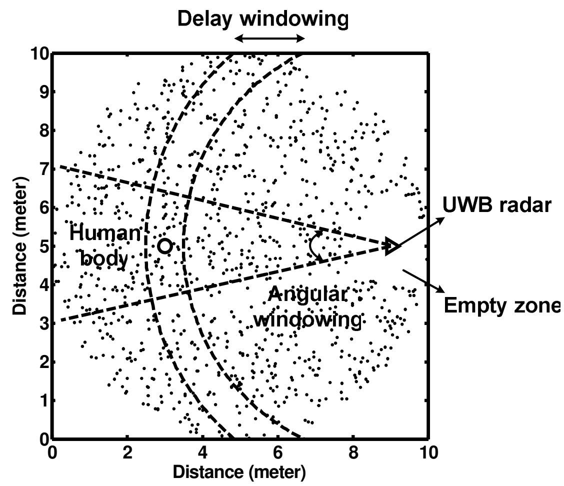

Fig. 1. Model constellation.

II. Geometry-Based Statistical Channel Model

The proposed model embodies two portions: a geometric channel model (GCM) that assumes certain distribution of scattering elements around the two ends of the radio connection, and a statistical tapped-delay-line (TDL) model that is derived from the GCM.

A. Geometric Model

As illustrated in Fig. 1, a large number of scatterers are randomly disposed in an azimuthally uniform fashion about a central location. The area containing the scatterers has a circular outer boundary and the radius of the circles defines the size of the service region. The human body is modeled as a scatterer and is deterministically positioned in the region. The radar is located in the region with a circular empty about the antenna. The empty zone serves to remove the antenna from immediate proximity to any scatterers which might overwhelm the effect of other scatterers [4].

The radar transmits UWB signals, which impinge on each of the scattering objects and are reflected off the targets. The backscatter signal is then received by the radar for further processing. It is assumed that each scatterer (including the human body) is an omnidirectional re-radiating element whereby the plane wave, on arrival, is reflected directly to the radar without the influence from other scatterers. Furthermore, the scatterers are assigned equal reflection coefficients and the path-loss exponent is 2. The antenna beam pattern may be made directional, which is simulated by the deletion from the constellation of any scatterers not contained within the antenna beam sector.

Assuming that the nominal location of the chest cavity of the human object is $\mathbf{x}_h$ and the location of the radar is $\mathbf{x}_r$, the signal arriving at the radar after reflection at the chest cavity travels a nominal distance $\|\mathbf{x}_h - \mathbf{x}_r\|$. Due to the periodical respiratory activity, the actual distance traveled by the multipath component (MPC) varies periodically about the nominal distance

$$d_0(t) = 2\|\mathbf{x}_h - \mathbf{x}_r\| + \Delta d_0 \cdot \cos(2\pi f_0 t) \tag{1}$$

where Δd_0 represents the maximum deviation in the distance traveled by the relevant MPC and f_0 is the respiration rate. Consequently, the path delay of the breathing signal is

$$\begin{aligned}\tau_0(t) &= \frac{d_0(t)}{c} = \frac{2\|\mathbf{x}_h - \mathbf{x}_r\| + \Delta d_0 \cdot \cos(2\pi f_0 t)}{c} \\ &= \tau_0 + \Delta\tau_0 \cdot \cos(2\pi f_0 t)\end{aligned} \tag{2}$$

where c is the speed of electromagnetic waves. We will assume that the channel is stationary besides the variations caused by human respiration. The generalized channel impulse response can thus be written as

$$\begin{aligned}h(t,\tau) &= \underbrace{\sum_j \alpha_j u(\tau - \tau_j)}_{\text{Stationary channel}} + \underbrace{\alpha_0 u(\tau - \tau_0(t))}_{\substack{\text{Time-varying channel} \\ \text{due to human respiration}}} \\ &\propto \sum_j \beta_j (d_j)^{-1} u\left(\tau - \frac{d_j}{c}\right) + \beta_0 (d_0(t))^{-1} u(\tau - \tau_0(t))\end{aligned} \tag{3}$$

where

α_j/α_0 = amplitude of the jth scatterer/breathing signal
$u(\cdot)$ = transmitted UWB pulse
τ_j = propagation delay of the jth scatterer
β_j/β_0 = $\{\pm 1\}$, phase shift of the jth scatterer/breathing signal
d_j = twice of the distance from the jth scatterer to radar

B. Statistical TDL Model

In real-life measurements, implicit band-limiting occurs in different components of the transmitting/receiving system. This band-limiting combines the MPCs so that resolving all of them is not possible. The minimum resolvable delay bin is proportional to the duration of the sounding pulse in the general case. Therefore, the channel impulse response expressed in (3) should be reformulated as

$$\begin{aligned}\tilde{h}(t,\tau) &= \sum_{\substack{i=1,\\ i\neq k}}^{I} \tilde{\alpha}_i u(\tau - \tilde{\tau}_i) + \tilde{\alpha}_k u(\tau - \tilde{\tau}_k(t)) = \sum_{\substack{i=1,\\ i\neq k}}^{I} \tilde{\alpha}_i u(\tau - i \times \delta\tau - \varepsilon_i) \\ &\quad + \tilde{\alpha}_k u(\tau - k \times \delta\tau - \Delta\tau_0 \cdot \cos(2\pi f_0 t) - \varepsilon_k)\end{aligned} \tag{4}$$

where

$\tilde{\alpha}_i$ = amplitude of the ith *effective scatterer*, which represents the combination of signals from physical scatterers falling into the ith delay bin
$\tilde{\alpha}_k$ = amplitude of the breathing signal, which represents the combination of signals from physical scatterers (including human body) falling into the kth bin
$\tilde{\tau}_i / \tilde{\tau}_k$ = propagation delay of the ith/kth effective scatterer
$\delta\tau$ = minimum resolvable path delay
$\varepsilon_i/\varepsilon_k$ = time-of-arrival (TOA) uncertainty of the ith/kth effective scatterer

It is worth mentioning that dense multipath channels degrade the precision of TOA estimation by biasing pseudo-range measurements. To evaluate the TOA estimation uncertainty, we assume that the channel is the main source of errors and system contributions such as clock accuracy or sensitivity are not a concern in the UWB context [5]. The ray-tracing and measurement results presented in [5] indicated that, when there is a direct line-of-sight (LOS) between the transmitter and the receiver, the LOS path ranging error can be modeled as a zero-mean Gaussian distribution with a standard deviation varying from several millimeters to a few centimeters. For the problem of interest here, a similar ranging accuracy is expected as the coverage of UWB systems is confined within a room of small to medium size. Therefore, both ε_i and ε_k can be modeled as additive white Gaussian noise (AWGN) with standard deviations $\sigma_{\varepsilon,i}$ and $\sigma_{\varepsilon,k}$. On one hand, it is expected that there is a positive correlation between $\sigma_{\varepsilon,i}$ and the number of physical scatterers, n_i, falling into the ith delay bin. This is because more overlapping pulses will produce larger TOA estimation uncertainty to the receiver. On the other hand, a larger power of the ith effective scatterer, P_i, will lead to a smaller $\sigma_{\varepsilon,i}$. Subsequently we consider the following versatile variable-exponent function for $\sigma_{\varepsilon,i}$:

$$\sigma_{\varepsilon,i}(\kappa_i) = \begin{cases} \sigma_{\varepsilon,\max} - (\sigma_{\varepsilon,\max} - \sigma_{\varepsilon,\min}) \left(\dfrac{\kappa_{\max} - \kappa_i}{\kappa_{\max} - \kappa_{\min}} \right)^L, & \text{if } \kappa_{\min} \le \kappa_i \le \kappa_{\max} \\ \sigma_{\varepsilon,\max}, & \text{otherwise} \end{cases} \tag{5}$$

where $\kappa_i = n_i/P_i$ is the number of physical scatterers in the ith delay bin when the power is normalized to 1. $\sigma_{\varepsilon,\min}$ is the minimum standard deviation of the ranging error, which corresponds to the irreducible TOA uncertainty exclusively due to system imperfection such as clock inaccuracy or finite

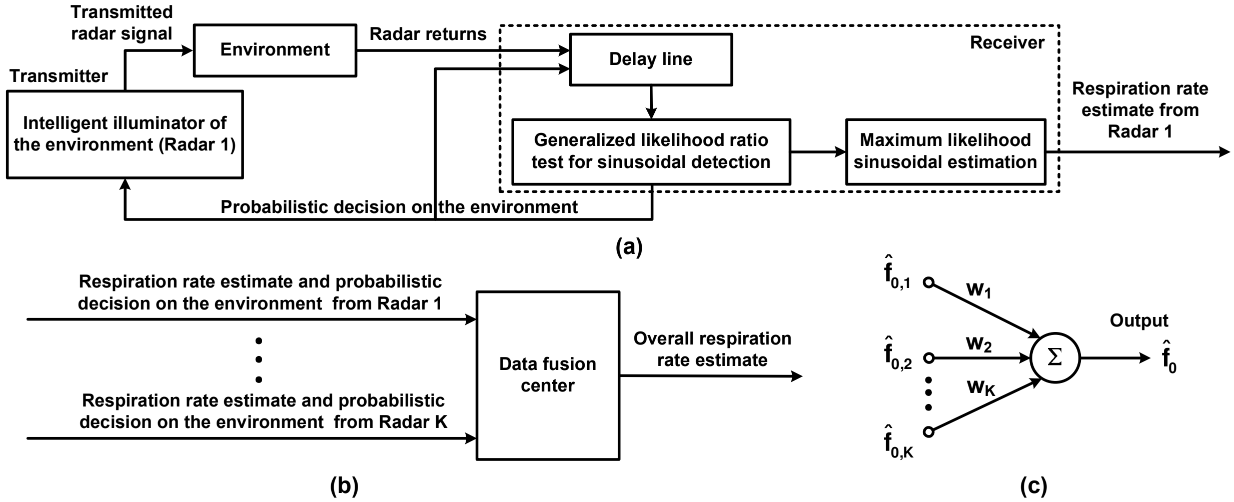

Fig. 2. System architecture of the UWB-DCRS: (a) block diagram of a single cognitive radar viewed as a dynamic closed-loop feedback system; (b) block diagram of a distributed radar system combining the recorded data from K cognitive radars; (c) data fusion center viewed as a linear combiner.

sensitivity. On the other hand, the maximum standard deviation of uncertainty, $\sigma_{\varepsilon,\max}$, is determined by the length of the delay bin, which is resulted when the normalized number of scatterers is not less than a threshold value $\kappa_{\max}$. The scale parameter L determines the sensitivity of $\sigma_{\varepsilon,i}$ with respect to the normalized number of scatterers κ_i.

In real-life applications, repetitive UWB pulses are transmitted to probe the channel. The pulse repetition frequency affects unambiguous range of the radar (which should be larger than the channel delay spread) and single pulmonary-activity measurement time (which should be at least 5 times shorter than the breathing period). Therefore, we are recording the received waveforms at discrete instants in slow time $t = mT_s$, ($m = 0, 1, \cdots, M$-1):

$$\begin{aligned}\tilde{h}\left(mT_s,\tau\right) &= \sum_{\substack{i=1,\\ i\neq k}}^{I}\tilde{\alpha}_i u\left(\tau - i\times\delta\tau - \varepsilon_i\left(mT_s\right)\right)\\ &+\tilde{\alpha}_k u\left(\tau - k\times\delta\tau - \Delta\tau_0\cdot\cos\left(2\pi f_0\times mT_s\right) - \varepsilon_k\left(mT_s\right)\right)\end{aligned} \tag{6}$$

where T_s represents the pulse repetition period. The TOA information can then be extracted at the receiver by applying various TOA estimation algorithms.

III. UWB-DCRS Architecture and Formulation of the Respiration-Rate-Estimation Problem

As presented in [6], a cognitive radar continuously interacts with the environment and, in a corresponding way, recursively updates the receiver with relevant environmental details. The adaptivity is extended to the transmitter such that it adjusts its illumination of the environment in an intelligent manner. Therefore, the cognitive cycle constitutes a dynamic closed-loop feedback encompassing the transmitter, environment, and receiver. In this section, we apply the idea of cognitive radar to a distributed sensing system to enhance the measurement reliability and, possibly, introduce multilevel intelligence in future implementation. The architecture of a UWB-DCRS is depicted in Fig. 2 and the details of each module are given as follows.

1) Transmitter

The transmitter is scanning the environment by either mechanically rotating a directional antenna with pencil beam or electrically beam-steering (see also Fig. 1). There are two main advantages of employing directional beam at the transmitter. Firstly, angular windowing ensures that only pulses backscattered from a certain direction are received, which makes TOA extraction less computationally-intensive. Secondly, by truncating the multipath profile in the angular domain, the number of overlapping pulses falling into the same delay bin may be reduced. This would lead to a more accurate respiration-rate estimate.

The tuning of antenna look-angles is automated by the probabilistic decision on the environment feedback from the receiver as depicted in Fig. 2(a). The goal is to rotate the directional beam until a well-formed breathing signal can be detected. It is worth mentioning that the tuning process involves a serial search of different windows (look-angles) until the correct window is acquired. It is important to use an *intelligent* search order to test windows based on the channel conditions (e.g., location and movements of the human body), which would give rise to more efficient signal acquisition.

2) Delay Line

The delay-line is used for controlling the sampling of the received echoes at the receiver. The receiver is only activated at very short time intervals triggered by the delay-line (delay windowing, see also Fig. 1). Thus, the length of the delay-line ensures that only pulses backscattered from a certain distance are received. Similar with angular windowing, the delay-line is controlled by the probabilistic decision on the environment feedback from the receiver such that the receiver is activated only if echoes from the chest wall are expected. Again, an optimum search order should be found to reduce the acquisition time.

3) Generalized Likelihood Ratio Test (GLRT) and Maximum Likelihood Estimate (MLE)

The process of target detection is part and parcel of the cognitive cycle. Firstly, it is recognized that the detection of chest-cavity movement corresponds to the detection of a sinusoid in AWGN following from the discussions in Section II. If we remove the two time-invariant terms $i \times \delta\tau$ and $k \times \delta\tau$ from (6) by assuming that they can be accurately computed as the average of all TOA estimates along slow-time mT_s, the general detection problem is (cf. Eq. (6))

$$\begin{cases} \mathcal{H}_0 : x[m] = \varepsilon[m], & m = 0,1,\cdots M-1 \\ \mathcal{H}_1 : x[m] = \Delta\tau_0 \cdot \cos\left(2\pi \bar{f}_0 m\right) + \varepsilon[m], & m = 0,1,\cdots M-1 \end{cases} \quad (7)$$

We model the detection problem as one of choosing between $\mathcal{H}_0$, which is termed the noise-only hypothesis, and $\mathcal{H}_1$, which is the signal-present hypothesis. $\varepsilon[m]$ is AWGN with known variance σ_ε^2, representing the TOA estimation uncertainty. $\bar{f}_0 = f_0 T_s$ denotes the normalized respiration rate. The observation interval is [0, M-1] with M denoting the signal length. If $\bar{f}_0$ is unknown to the receiver, it can be shown that the GLRT decides $\mathcal{H}_1$ if

$$\max_{\bar{f}_0} I\left(\bar{f}_0\right) > \gamma \quad (8)$$

Where $I\left(\bar{f}_0\right)$ is the periodogram [7]. γ is the detection threshold. The detector decides that a sinusoid is present if the peak value of the periodogram exceeds a threshold. The relationship between probability of detection P_D and probability of false alarm P_{FA} can be found as [7]

$$P_D = \int_{2\ln\frac{M/2-1}{P_{FA}}}^{\infty} p(y)\,dy \quad (9)$$

The random variable $y \sim \chi_2'^2\left(M\Delta\tau_0^2 / 2\sigma_\varepsilon^2\right)$ with $\chi_2'^2(\lambda)$ being the noncentral chi-squared probability density function (pdf) with two degrees of freedom and noncentrality parameter λ. $p(y)$ denotes the corresponding noncentral chi-squared pdf.

If the unequality condition in (8) is satisfied, the frequency location of the peak of the periodogram, $\hat{f}_0$, is the MLE of the frequency. The MLE achieves the Cramer-Rao lower bound (CRLB) asymptotically, which can be evaluated as

$$\operatorname{var}\left(\hat{f}_0\right) \to \frac{6\sigma_\varepsilon^2}{\pi^2 \Delta\tau_0^2 M (M-1)} \quad (10)$$

where var(·) denotes the variation of the estimate.

4) Data Fusion Center

To provide more robust and accurate breathing signal estimation, a distributed radar system is implemented as depicted in Fig. 2(b). K cognitive radars are deployed in a service region to monitor the pulmonary activity. All of them are linked to a data fusion center, where the frequency estimates from various radars are processed coherently to yield the overall respiration rate estimate.

For the sake of simplicity, we consider a linear combiner as illustrated in Fig. 2(c), which consists of a set of adjustable weights connected to input terminals. The overall estimate is computed as

$$\hat{f}_0 = \sum_{k=1}^{K} w_k \hat{f}_{0,k} \quad (11)$$

where w_k is the weight associated with the kth cognitive radar and $\hat{f}_{0,k}$ is the corresponding respiration rate estimate. The weights are controlled by the probabilistic decision on the environment. In general, there are two criteria for defining the weighs.

1) Reliability-based combining

$$w_k = \mathcal{F}\left(P_{D,k}\right) \text{ subject to } \sum_{k=1}^{K} w_k = 1 \quad (12)$$

In Eq. (12), $P_{D,k}$ is the probability of detection for the kth sensor (cf. (9)). The bijection $\mathcal{F}$ is monotonically nondecreasing, which indicates that this combination scheme favors a "more reliable" radar.

2) Signal-variance-based combining

$$w_k = \mathcal{G}\left(\operatorname{var}\left(\hat{f}_{0,k}\right)\right) \text{ subject to } \sum_{k=1}^{K} w_k = 1 \quad (13)$$

where $\operatorname{var}\left(\hat{f}_{0,k}\right)$ is the variance of frequency estimate from the kth radar. The bijective function $\mathcal{G}$ is monotonically nonincreasing. Therefore, an estimate with smaller variance is weighted more heavily.

V. Conclusion

We have demonstrated the use of UWB radar in non-contact monitoring of respiration rates. This technology shows promise in various medical and security applications. A geometry-based statistical channel model has been developed for simulating the time-varying multipath profiles due to the pulmonary activity. We have also developed the UWB-DCRS for the robust detection of chest cavity motion and the accurate estimation of respiration rate.

References

[1] A. N. Vgontzas and A. Kales, "Sleep and its disorders," *Annu. Rev. Medicine,* vol. 50, pp. 387-400, 1999.

[2] E. M. Staderini, "UWB radars in medicine," *IEEE Aerospace and Electronic Systems Magazine,* vol. 17, pp. 13-18, Jan. 2002.

[3] I. Y. Immoreev, S. Samkov, and T. H. Tao, "Short-distance ultra wideband radars," *IEEE Aerospace and Electronic Systems Magazine,* vol. 20, pp. 9-14, June 2005.

[4] F. Amoroso and W. W. Jones, "Geometric model for DSPN satellite reception in the dense scatterer mobile environment," *IEEE Trans. Commun.,* vol. 41, pp. 450-453, Mar. 1993.

[5] B. Alavi and K. Pahlavan, "Bandwidth effect on distance error modelling for indoor geolacation," in *Proc. IEEE PIMRC 2003,* vol. 3, pp. 2198-2202, Sept. 2003.

[6] S. Haykin, "Cognitive radar: A way of the future," *IEEE Signal Processing Mag.,* vol. 23, pp. 18-29, Jan. 2006.

[7] S. M. Kay, *Fundamentals of Statistical Signal Processing: Detection Theory*, PTR Prentice-Hall Inc., 1998.